

Contents lists available at ScienceDirect

Journal of Non-Crystalline Solids

journal homepage: www.elsevier.com/locate/jnoncrysol



Packing fractions in borate and silicate glasses with an emphasis on lead and bismuth systems

Keya Aggarwal ^{a, b}, Steve Feller ^{a, *}

- a Department of Physics, Coe College, Cedar Rapids, IA 52402, USA
- ^b Welham Girls' School, Dehradun, Uttarakhand 248001, India

ARTICLE INFO

Keywords: Density

Glasses

Borate Silicate

Packing

Structure

ABSTRACT

The densities of lead oxide and bismuth oxide modified glasses determined over a wide range of compositions were collected from the literature. Using these data as well as Shannon atomic radii and atomic masses, the glass systems' total packing fractions and oxygen packing fractions were computed. For borates, these fractions were correlated against the trend of the fraction of tetrahedral borate (N_4) units. This analysis was compared to that of lithium borate and silicate glasses and zinc borate glasses. The peak of the N_4 distribution versus R (= molar fraction of modifier/molar fraction B_2O_3) corresponds well to the peak in oxygen packing in lithium and lead borate glasses but does not closely coincide with the peak in oxygen packing for zinc and bismuth glasses. In contrast to the borates, silicon in glassy silicate systems does not change coordination and the resulting packing trends change less than in the borates. Furthermore, the packing in the silicate systems is correlated to the change in Q_n units.

1. Introduction

Borate and silicate glasses contain well-defined short-range order atomic structures which alter their densities as a function of composition. In comparison to molar volumes, which vary strongly with a change in metal modifier, the packing fractions for the same glass formers follow trends that are, in many cases, nearly independent of the modifying species. This suggests that packing is a more universal and reliable concept, hence it provides the perspective of a unitless density [1–4].

Packing can be generalized into two types: ionic and covalent, based on the comparison of the volume of the modifier to network-forming oxygen [4,5]. Glasses that have a modifier with a radius equal to or smaller than oxygen exhibit covalent packing. This type of packing is characterized by a lower efficiency in terms of how the atoms fit together, primarily because of the strong network-building capability of covalent oxygen. The packing fractions of these glasses clearly portray the underlying atomic structure where borate packing increases with the change from 3 to 4 coordination and silicates show a consistent evolution of the $Q_{\rm n}$ units, where $Q_{\rm n}$ is a silicon tetrahedron with n bridging oxygens. On the other hand, ionic packing pertains to glasses in which the modifier has a significantly larger radius than that of oxygen. This

In this paper, the packing fraction of lithium, zinc, bismuth and lead borate as well as lithium, bismuth and lead silicate glass systems have been calculated and the resulting trends are discussed. In all cases in this paper, covalent packing was observed.

2. Choice of radius [6]

The radii chosen for the calculations of the packing fraction are the Shannon crystal radii [7]. The choice of Shannon radii has been made for volume calculations as they represent the most accurately known ionic and crystal radii and have been corrected for the first shell coordination number. Crystal radius was chosen over ionic radius for the calculations due to the following three arguments:

2.1. Geometric argument for borate glasses

An unmodified borate glass has a trigonal planar structure where we can assume that the oxygens touch each other to form an equilateral

E-mail address: SFELLER@COE.EDU (S. Feller).

arrangement tends to have greater packing efficiency. The ionic packing trends appear to be dominated by random packing of hard metallic ionic spheres, supportive of the idea that these ions control the filling of space, especially at large molar fractions of modifying oxide [4,5].

 $^{^{\}ast}$ Corresponding author.

triangle due to the negligible volume of boron (refer to Table 1). The center-to-corner distance is equal to the boron-to-oxygen (B–O) bond length of $1.36\,\text{ Å}$ in both the glass and the crystal [7,8]. Using the properties of cosines, we can solve for the radius of oxygen using a right triangle where the hypotenuse is the B-O bond length and the adjacent side is the radius of oxygen with a 30° angle in between. This radius needs to be $1.18\,\text{ Å}$ to fit this triangle. This is closest to the Shannon crystal radius of oxygen of $1.21\,\text{ Å}$ [7]. However, the ionic radius of $1.35\,\text{ Å}$ [7] for O from Shannon produces an edge length of $2.70\,\text{ Å}$ which is extremely inaccurate in comparison to the edge length of $2.40\,\text{ Å}$ [8] determined from neutron diffraction, proving the comparative accuracy of the crystal radius. To use a consistent set of radii, analyses of the silicate systems were done with the same choice of crystal radii.

2.2. The boron oxide packing argument-

Packing fractions using both crystal and ionic radii of pure boron oxide glass are found to be quite different [6]. The ratio of the packing fraction of crystalline and glassy B_2O_3 should be equal to the corresponding ratio of the densities(1.81/2.46 = 0.736) since this represents an efficiency of packing of the same number and kinds of atoms. For glassy B_2O_3 to achieve its known density of 1.81 g/cc³ [18], we expect a packing fraction of the glass to be 0.362 based on a crystallographic value of the packing fraction in B_2O_3 of 0.492 [6] (0.736×0.492=0.362). The packing fraction calculated using crystal radii, 0.349, is significantly closer to the expected packing fraction of 0.362 than that calculated using ionic radii, 0.484 [7].

2.3. The consistency argument-

Crystal radii show a clear and consistent relationship between ionic size and packing in both borate and silicate-based glasses, with larger modifiers having higher packing fractions (ionic packing) and smaller modifiers having lower packing fractions (covalent packing). Ionic radii, on the other hand, do not exhibit this predictable trend and introduce inconsistencies [6].

3. Calculation of packing fraction

Packing fraction (PF) is the ratio of the volume of the constituent atoms in a mole to the total molar volume of the glass-forming system. It is calculated using:

$$PF = \left(\sum \left(4/3\pi r_i^3 n_i\right) * N_A / V_m\right) \tag{1}$$

Where V_m is the molar volume calculated using the formula:

$$V_m = M(x)/\rho(x) \tag{2}$$

M(x) is the molar mass, $\rho(x)$ is the density, r_i is the radius of the constituent atom, n_i is the number of that corresponding atom present in the structural formula and N_A is Avagadro's number. Table 1 lists the needed radii and consequent volumes.

This paper uses R for the compositional notation instead of x, the molar fraction of the modifier to represent packing fractions as it ensures a comparatively linearized structural trend. For example, if the lithium borate glass system is represented using the x notation as $xLi_2O.(1-x)$ B_2O_3 , using the R notation, it shall be represented by $RLi_2O.$ B_2O_3 .

$$Thus, R = x/(1-x) \tag{3}$$

4. Packing in borate glass systems

4.1. Packing in the lithium borate glass system [4-6,9-39]

Glasses of the borate systems show both 3 and 4 coordination for boron [9–39]. While boron in vitreous B_2O_3 is trigonal planar, as the content of the alkali increases (for approximately 0 < R < 0.7) four-coordinated tetrahedral borons replace the planar units. On further increase in alkali content, the tetrahedral units get converted back to planar units with an increasing number of non-bridging oxygens. This continues until the end of the glass forming range near R = 3 at which point each boron is bonded to three non-bridging oxygens [40].

This structural evolution is consistent with the packing trend for the lithium borate glass systems as evident in Figs. 1 & 2. For this (and all other) systems, the oxygen packing fraction is calculated along with the packing fraction for the entire system; oxygen packing is found by setting the radii of all atoms to zero except for that of oxygen. The increasing trend of the total packing fraction is consistent with that of tetrahedral boron fraction, both peaking at around R=0.7. After the peak, the packing fraction and N_4 decreases and the extra oxygens from the lithium oxide are accommodated by an increasing number of non-bridging oxygens in the borate system.

As is apparent from the graphical representations, the trend of the tetrahedral boron fraction more closely aligns with the oxygen packing fraction than with the overall system packing fraction. This is due to the dominance of oxygen over boron in the system due to the large difference in the volumes and the lack of contribution of lithium to the atomic structure of the network (represented in Table 1).

4.2. Packing in the zinc borate glass system [6,41-44]

In the zinc borate glass system (plotted in Figs. 3 & 4), the packing

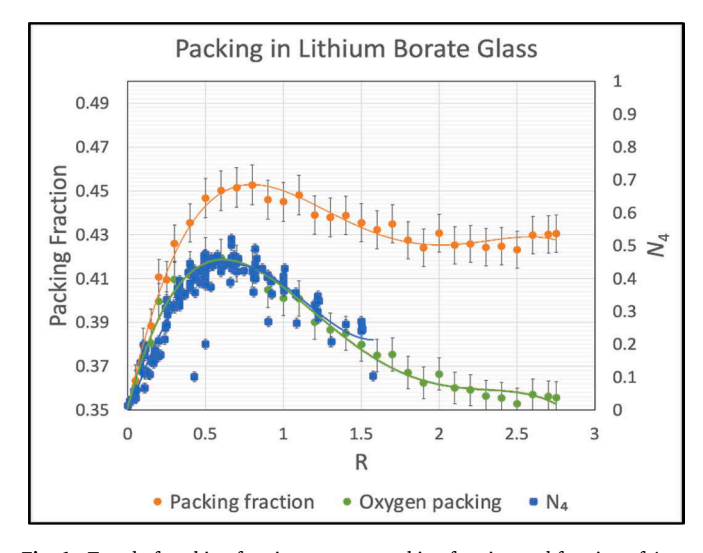


Fig. 1. Trend of packing fraction, oxygen packing fraction and fraction of 4-co-ordinated boron in lithium borate glass systems.

Table 1The radii and volume of ions and atoms used in the packing fraction calculations [7].

Name	Boron	Silicon	Lithium	Oxygen	Zinc	Bismuth	Lead
Radius	0.15Å	0.40Å	0.73Å	1.21Å	0.74Å	1.14Å*	1.12Å
Volume	0.014Å ³	0.27Å ³	1.6ų	7.41Å ³	1.7Å ³	6.2Å ³	5.9Å ³

^{*} The value 1.14 Å was chosen as the average of the 5 and 6 coordinated bismuth which is from the crystal structure of room temperature Bi₂O₃ which are 1.1 and 1.17 respectively [7].

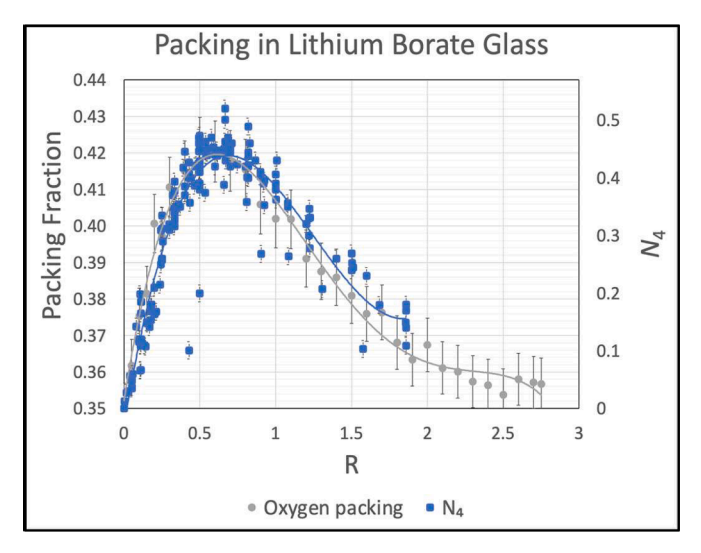


Fig. 2. Detailed trend of oxygen packing fraction and fraction of 4-coordinated boron in lithium borate glass systems.

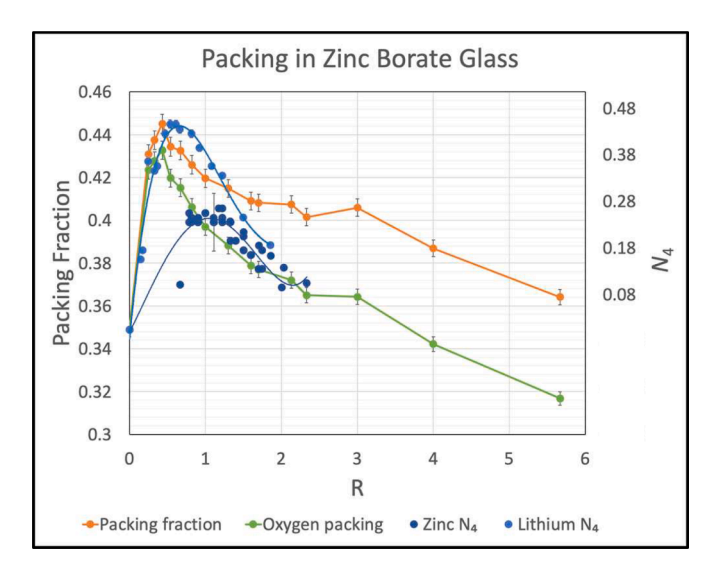


Fig. 3. Trend of packing fraction, oxygen packing fraction and N_4 of zinc borate glasses. Also plots N_4 of lithium borate glasses.

trend exhibits a pronounced rise and has a maximum at approximately R=0.5, followed by a gradual descent. Notably, the N_4 metric more closely mirrors the oxygen packing rather than the actual packing fraction due to the domination of the oxygen volume in this system as well.

Upon closer examination of the graphical representation, it becomes evident that there is a correlation between the fraction of four-coordinated borates with the packing fraction in the range spanning from R=1 to 2.25. However, establishing a definitive trend is a challenging task due to the absence of any prior research concerning both lower and higher values of zinc borate N_4 due to phase separation and crystallization. Additional research with rapid cooling is imperative to fill this knowledge gap. Consequently, the peak cannot be unequivocally established, and the relationship remains unsubstantiated since the slope can be influenced by the chosen scale.

It is important to establish that the fraction of tetrahedral borons in the zinc-modified and lithium-modified borate glass systems are not synonymous, despite their nearly identical atomic volumes (refer to Table 1 and Fig. 3).

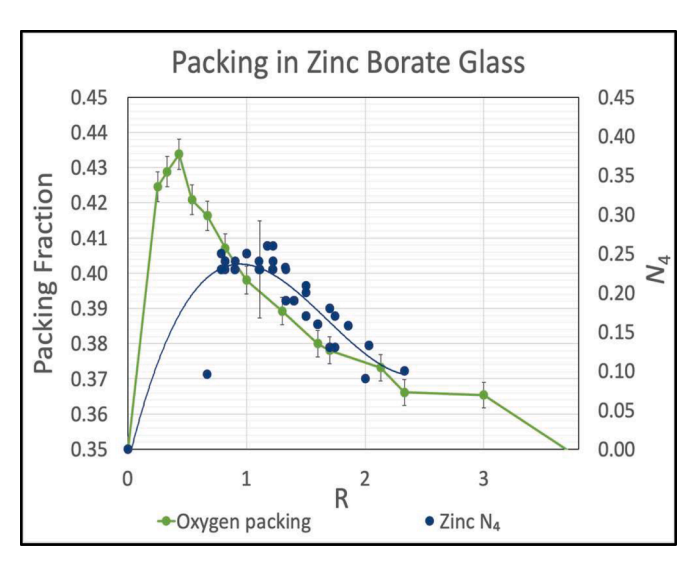


Fig. 4. Detailed trend of oxygen packing fraction and fraction of 4-coordinated boron in the zinc borate glass system.

4.3. Packing in the lead borate glass system [32,43,45-57]

In the lead borate glass system (Fig. 5) packing peaks at around R = 0.45. As the radius of lead is comparable to that of oxygen, the fraction of the four-coordinated boron (N₄) corresponds more closely with the total packing fraction than the oxygen packing as seen for earlier systems. The plots display a spread of N₄ for the same values of R due to the errors from the formation and measurement of the glasses and the measurement of N₄ by different means and groups.

Recent Raman and NMR studies [49] reveal a transition in lead's chemical bonding behavior from predominantly ionic to covalent when R exceeds 1.5. While this transition will not alter the maxima of the plotted packing curve, it could affect the high R part of the plot in proportion to the ratio of the lead atoms exhibiting this transition which is still under study. Fig. 5 is plotted under the assumption that all the lead atoms are ionic and the Shannon crystal radius is used.

4.4. Packing in the bismuth borate glass system [58-62]

In bismuth borate glasses, the packing data peaks at around R=0.26 and the fraction of four coordinated borons peaks at around R=0.8 (Fig. 6). However, it's important to note that the paucity of data for N_4

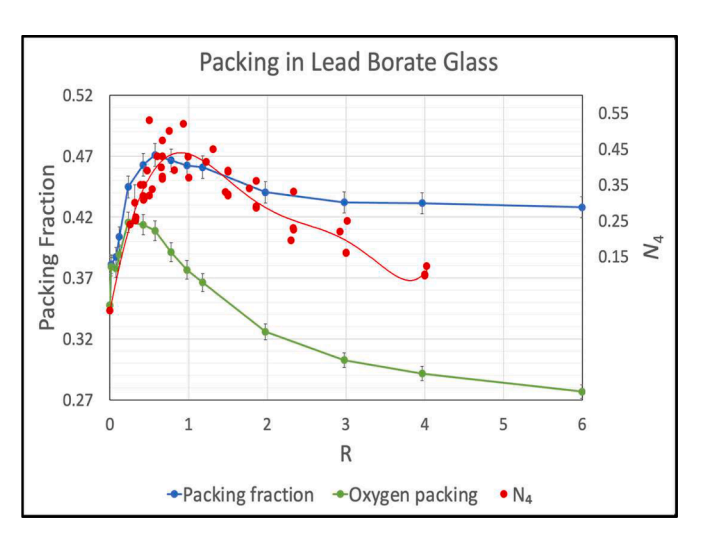


Fig. 5. Trend of packing fraction, oxygen packing fraction and N_4 of lead borate glasses.

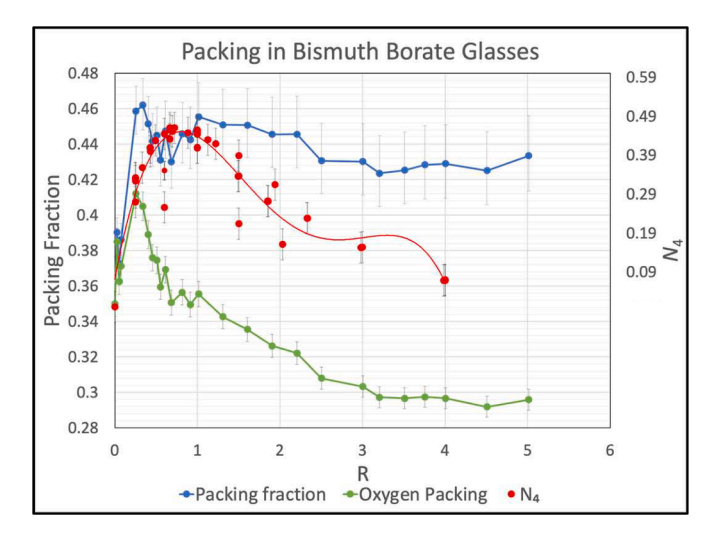


Fig. 6. Trend of packing fraction, oxygen packing fraction and N_4 of bismuth borate glasses.

units in this system for higher R values hinders the accuracy of the trendline which makes the determination of trends difficult.

5. Packing in silicate glass systems

Similar to the borate glasses, the silicates show two groups of systems based on the radii of the modifiers. The packing trends initially increase monotonically as a function of modifier content. Silicates only exist as tetrahedra in the glass systems studied here. The covalent packing of small modifiers in silicate glasses is demonstrative of the evolution of the $Q_{\rm n}$ units.

5.1. Packing in the lithium silicate glass system [63–66]

The lithium oxide-modified silicate glass system in Fig. 7 exhibits a continuous increase in its packing, albeit with a reduced rate of change beyond $R \approx 0.5$. Here R is the molar ratio of the modifier to silica. In contrast, we observe a distinct decrease in the oxygen packing. This phenomenon arises due to the rising number of non-bridging oxygens (NBO) resulting from an increased modifier content. The increase in the NBOs results in an accumulation of negative charge, see Fig. 7, and

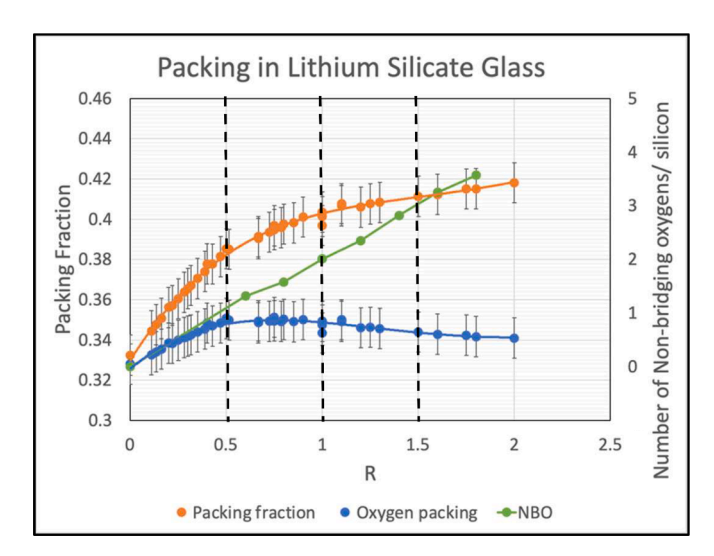


Fig. 7. Trend of packing fraction and oxygen packing fraction of lithium silicate glasses along with the number of non-bridging oxygens per silicon [65]. The dashed vertical lines represent the transition points of the Q_n units.

disrupts the interconnected tetrahedra of the original silicate glass. While the overall packing still increases due to the modifier, it does so at a slower rate due to the formation of the NBOs. It appears that the Q_n units cause changes in the slope of the packing curve near the transition points of the Q_n groups, see Table 2 and Fig. 7.

When comparing the packing of lithium silicates to lithium borates in Fig. 8, we can observe a monotonic trend in the packing of silicates due to a lack of coordination changes. The slope appears to change at each transition point for the formation of Q_{n-1} from Q_n that is at $R=0.5,\,1,\,1.5,\,$ and 2 (see Table 2 and Fig. 7). Moreover, at higher R values, the packing of the silicate system begins to approach that of the borate system. This alignment serves as a self-consistency test. At lower R values, the packing differs due to the configuration of borates (forming tetrahedral units from trigonal borates) and silicates (forming non-bridging oxygens on silicate tetrahedra), but at higher R values, the system predominantly consists of Li₂O, rather than silicate or borate units, as the composition gradually tends toward being nearly Li₂O.

5.2. Packing in the lead silicate glass system [66-68]

The packing behavior in lead silicates is different than the trend observed in the lithium-silicate system. The decrease in the lead silicate packing fraction and oxygen packing fraction can be attributed to the increase in the number of non-bridging oxygens per silicon as evident in Fig. 9.

Fig. 10 compares the packing in lead silicate and borate glasses. We observe a strong peak in the packing fraction in the lead borate glass system due to the presence of the tetrahedral borons. The lead silicates show less change in the packing trend compared to borates due to the lack of coordination change of the silicon. Silicon undergoes Q_n unit changes as NBOs are added to the silica tetrahedra. As in the lithium silicates, the lead silicates follow a similar change in the volume of the Q_n units (see Table 2). The volumes of the Q_n units increase as R increases.

As R increases past about 1.5 lead changes from ionic to covalent character. However, we continue to use Shannon's crystal radii since no evident change in trend was seen.

It appears that at high R, the packing of the lead borate and silicate systems becomes comparable; this is another example of the consistency

5.3. Packing in the bismuth silicate glass system [66]

The bismuth silicate glass system (as represented in Figs. 11 & 12) portrays anomalous packing behavior. The increase in NBO formation has not been experimentally deduced, however, it may be inferred by assuming that the oxygen from bismuth oxide creates non-bridging oxygens on the silicon tetrahedra (see Fig. 11). Unlike the typical silicate glass system behavior that demonstrates a relatively uniform packing fraction trend, this system portrays a dip in the packing at around R=0.67. The composition of the glass is written by RBi₂O₃. SiO₂. For this system, let us assume that the initial addition (R<=0.67) of bismuth oxide modifies the SiO₂ glass network by forming non-bridging oxygens; in the borates initial addition of bismuth oxide causes the borate network to be modified with the formation of tetrahedral boron. Then, for the silicate case, the Q_n units will occur at R values one third that of lithium or lead silicates (see Table 2) since 3 oxygens come in for each formula unit of Bi₂O₃. These compositions are shown in Table 3.

The packing trend appears to exhibit effects due to the compositional trend of the Q_n units. No single-phase glasses are produced for $R\!<\!0.33$.

Table 2 Compositions for the Q_n units in lithium and lead silicate glasses.

Q _n units	Q_4	Q_3	Q_2	Q_1	Q_0
R	0	0.50	1.00	1.50	2.00

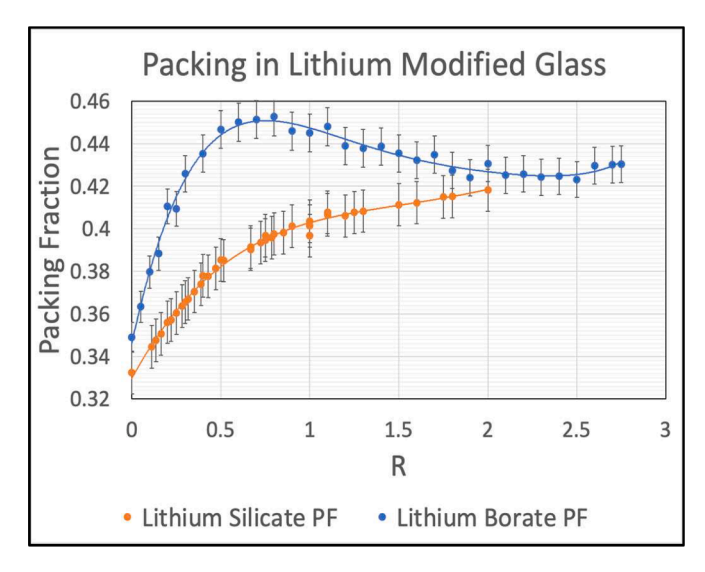


Fig. 8. Trend of lithium silicate and lithium borate packing fraction.

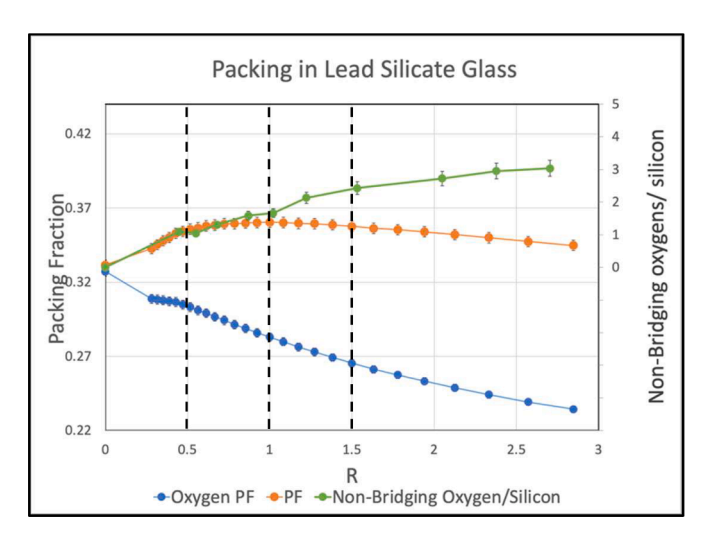


Fig. 9. Trend of packing fraction and oxygen packing fraction of lead silicate glasses along with the number of non-bridging oxygens per silicon [67]. The error in the oxygen packing is smaller than the symbol size. The dashed vertical lines represent the transition points of the Q_n units.

Thus, the conversion from Q_4 to Q_3 and from Q_3 to Q_2 is not seen in the packing trend (see Fig. 11). Near R=0.33 single-phase glass formation commences, and the packing is consistent with a glass mostly composed of Q_2 units. Near R=0.5 the packing trend reaches a local maximum indicative of the completed conversion of Q_2 to Q_1 . For R>0.5 and R<0.67, Q_1 converts to Q_0 . This is seen as a local minimum in the packing trend. Above R=0.67, the silicate network no longer changes and the overall packing trends towards that of crystalline Bi_2O_3 . The density of crystalline Bi_2O_3 is 8.9 g/cc [69,70]. Using the atomic masses of Bi and O and the relevant Shannon radii (see Table 1), the packing of crystalline Bi_2O_3 was found to be 0.40. The packing trend of the bismuth silicate glasses was found to asymptotically approach that of crystalline Bi_2O_3 (see Fig. 11).

Fig. 12 compares the packing of bismuth silicate and borate glasses. The packing of the borate system is considerably higher than that of the silicate system. This is indicative of the formation of boron tetrahedra. The N_4 has a maximum around R=0.8, whereas the packing has a maximum near R=0.26 (see Fig. 6). If bismuth oxide modifies boron oxide, a unit change in R produces 3 added oxygens to the borate network. Thus, the composition for the maximum in N_4 should be

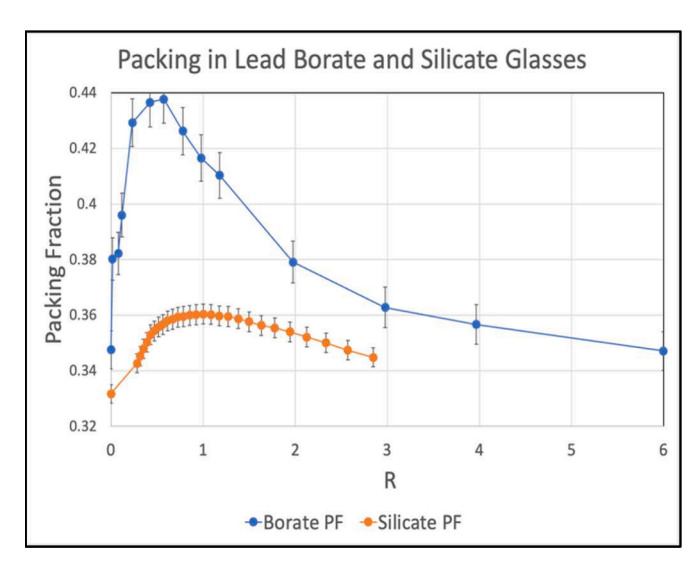


Fig. 10. Trend of lead silicate and lead borate packing fraction.

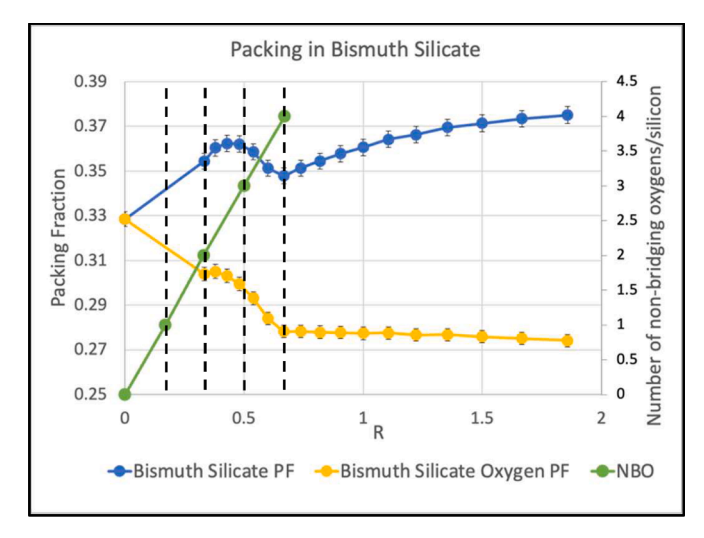


Fig. 11. Trend of packing fraction and oxygen packing fraction of bismuth silicate glasses along with the number of non-bridging oxygens per silicon inferred by assuming oxygens form non-bridging oxygens on the silicon tetrahedra. The dashed vertical lines represent the transition points of the Q_n units.

downshifted compared to the lithium and lead borate systems which add 1 oxygen per unit change in R. The peak in N_4 for the lithium borate system occurs near R=0.7 and for the lead system, it occurs near R=1. As a result, it appears that not all added oxygen is used to form N_4 in the bismuth borate glasses. The packing data at high R trends downward towards that of crystalline Bi_2O_3 but has sufficient scatter to not allow further speculation.

6. Conclusion

Packing fractions for lithium, zinc, lead and bismuth borate glasses as well as lithium, lead and bismuth silicate glasses were calculated, plotted, and analyzed. Packing was seen to be strongly influenced by the underlying atomic structure in these glass systems. In the borates packing is most affected by N_4 and in the silicates by the transition of the O_n units.

In particular, the oxygen packing in the lithium borate system most closely resembles N_4 as a function of composition. In zinc, lead, and bismuth borates, the correlation to N_4 is present but weaker. This is due, in part, to the scatter present in the data.

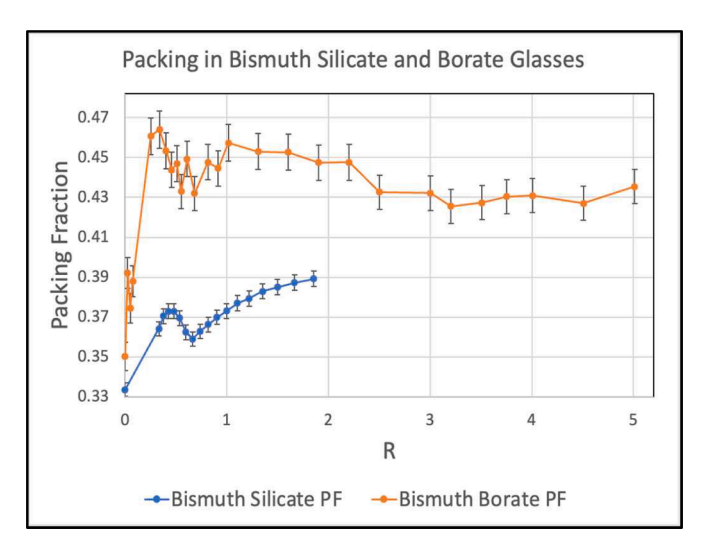


Fig. 12. Trend of bismuth silicate and bismuth borate packing fraction.

Table 3 Compositions for the Q_n units in bismuth silicate glasses.

Q _n units	Q ₄	Q_3	Q_2	Q_1	Q_0
R	0	0.17	0.33	0.50	0.67

In the silicates, the trend of the packing changes its slope near the transition points of Q_n to Q_{n-1} followed by Q_{n-1} to Q_{n-2} . The transition compositions for bismuth silicates occurs at R values one-third that of lithium and lead silicates. This is because Bi_2O_3 brings in 3 times as much oxygen as Li_2O or PBO per unit modifier. In bismuth silicates, this is clearly seen in the packing trends. Eqs. (1)–(3)

CRediT authorship contribution statement

Keya Aggarwal: Writing – review & editing, Writing – original draft, Visualization, Software, Methodology, Investigation, Formal analysis, Data curation, Conceptualization. **Steve Feller:** Writing – review & editing, Investigation, Conceptualization, Methodology, Validation, Resources, Supervision, Project administration, Funding acquisition.

Declaration of competing interest

The authors declare that they have no known competing financial interests or personal relationships that could have appeared to influence the work reported in this paper.

Data availability

Data will be made available on request.

Acknowledgments

I (KA) would like to express my deepest appreciation to my grand-father, Professor Arun Varshneya of Alfred University, Alfred NY for introducing me to glass science, and the Department of Science at Welham Girls' School, Dehradun (India) for their encouragement. The authors would also like to thank Ian Slagle of Georgia Tech for assistance with NMR measurements. We acknowledge the US National Science Foundation for assistance under grant number 2203142.

References

- A. Zeidler, P.S. Salmon, L.B. Skinner, Packing and the structural transformations in liquid and amorphous oxides from ambient to extreme conditions, Proc. Natl. Acad. Sci. 111 (28) (2014) 10045–10048.
- [2] U. Hoppe, A structural model for phosphate glasses, J. Non-Cryst. Solids 195 (1996) 138–147.
- [3] U. Hoppe, Behavior of the packing densities of alkali germanate glasses, J. Non-Cryst. Solids 248 (1999) 11–18.
- [4] S. Bista, A. O'Donovan-Zavada, T. Mullenbach, M. Franke, M. Affatigato, S. Feller, Packing in alkali and alkaline earth borosilicate glass systems, Phys. Chem. Glasses Eur. J. Glass Sci. Technol. B 50 (3) (2009) 224–228.
- [5] S.K. Giri, E.R. Hemesath, C.J. Olson, S.A. Feller, M. Affatigato, A study of packing in alkali borate glass systems, Phys. Chem. Glasses 44 (3) (2003) 230–233.
- [6] S. Weiss, P. McGuire, I. Slagle, J. Cook, S.A. Feller, Comparisons of atomic arrangements in binary borate glasses with total, oxygen and modifier packing fraction, Phys. Chem. Glasses Eur. J. Glass Sci. Technol. B 62 (3) (2021) 73–83.
- [7] Database of Ionic Radii, These radii were taken from Shannon, R. D. Revised effective ionic radii and systematic studies of interatomic distances in halides and chalcogenides, Acta Crystallogr. A32 (1976) 751–767 [accessed December 2023], https://abulafia.mt.ic.ac.uk/shannon/ptable.php.
- [8] A. Hannon, D.I. Grimley, R.A. Hulme, A.C. Wright, R.N. Sinclair, Boroxol groups in vitreous boron oxide: new evidence from neutron diffraction and inelastic neutron scattering studies, J. Non-Cryst. Solids 177 (2) (1994) 299–316.
- [9] S. Feller, J. Kottke, J. Welter, S. Nijhawan, R. Boekenhauer, H. Zhang, D. Feil, C. Parameswar, K. Budhwani, M. Affatigato, A. Bhatnagar, G. Bhasin, S. Bhowmik, J. Mackenzie, M. Royle, S. Kambeyanda, P. Pandikuthira, M. Sharma, Borate glasses, crystals and melts. Soc. Glass Technol. 1 (1997) 246–253.
- [10] W.H. Zachariasen, The crystal structure of lithium metaborate, Acta Crystallogr. 17 (6) (1964) 749.
- [11] P.J. Bray, J.G. O'keefe, Nuclear magnetic resonance investigations of the structure of alkali borate glasses, Phys. Chem. Glasses 4 (2) (1963) 37–46.
- [12] A.C. Wright, S.A. Feller, A.C. Hannon, Borate Glasses, Crystals and Melts, Society of Glass Technology, Sheffield, 1997.
- [13] G.E. Jellison Jr, S.A. Feller, P.J. Bray, A re-examination of the fraction of 4-coordinated boron atoms in the lithium borate glass system, Phys. Chem. Glasses 19 (3) (1978) 52–53. GB: DAVOLNOBIBL, 6 REF.
- [14] S.A. Feller, Lithium-7, boron-10, boron-11, and oxygen-17 nuclear magnetic resonance studies of lithium borate glasses and related compounds. Ph.D. Thesis Brown University (1980).
- [15] Y.H. Yun, P.J. Bray, B11 nuclear magnetic resonance studies of Li2O B2O3 glasses of high Li2O content, J. Non-Cryst. Solids 44 (2–3) (1981) 227–237.
- [16] P.J. Bray, Structural models for borate glasses, J. Non-Cryst. Solids 75 (1–3) (1985) 29–36.
- [17] J. Zhong, P.J. Bray, Change in boron coordination in alkali borate glasses, and mixed alkali effects, as elucidated by NMR, J. Non-Cryst. Solids 111 (1989) 67–76.
- [18] S. Prabakar, K.J. Rao, C.N.R. Rao, 11B NMR spectra and structure of boric oxide and alkali borate glasses, Proc. R. Soc. Lond. A Math. Phys. Sci. 429 (1876) (1990) 1–15
- [19] L. van Wüllen, W. Müller-Warmuth, 11B MAS NMR spectroscopy for characterizing the structure of glasses, Solid State Nucl. Magn. Reson. 2 (1993) 279–284.
- [20] P. Mustarelli, E. Quartarone, F. Benevelli, A 11b and 7LI MAS-NMR study of sol-gel lithium triborate glass subjected to thermal densification, Mater. Res. Bull. 32 (1997) 679–687.
- [21] M. Ganguli, K.J. Rao, Structural role of PbO in Li2O-PbO-B2O3 glasses, J. Solid State Chem. 145 (1) (1999) 65-76.
- [22] W.J. Clarida, J.R. Berryman, M. Affatigato, S.A. Feller, S.C. Kroeker, J. W. Zwanziger, B. Meyer, F. Borsa, S.W. Martin, Dependence of N4 upon alkali modifier in binary borate glasses, Phys. Chem. Glasses 44 (3) (2003) 215–217.
- [23] S. Kroeker, P.M. Aguiar, A. Cerquiera, J. Okoro, W. Clarida, J. Doerr, M. Olesiuk, G. Ongie, M. Affatigato, S.A. Feller, Alkali dependence of tetrahedral boron in alkali borate glasses, Phys. Chem. Glasses Eur. J. Glass Sci. Technol. Part B 47 (4) (2006) 393–396.
- [24] P.M. Aguiar, S. Kroeker, Boron speciation and non-bridging oxygens in high-alkali borate glasses, J. Non-Cryst. Solids 353 (18–21) (2007) 1834–1839, no.
- [25] V.M. Michaelis, P.M. Aguiar, S. Kroeker, Probing alkali coordination environments in alkali borate glasses by multinuclear magnetic resonance, J. Non-Cryst. Solids 353 (26) (2007) 2582–2590.
- [26] J. Maldonis, J. North, A. Ramm, D. Starkenburg, K. Hopkins, E. Wiese-Moore, P. Rasmussen D. Delgado, M. Affatigato, S.A. Feller, V.K. Michaelis, S. Kroeker, B. Dahal, B. Baker, U. Hoppe, Structure studies of caesium and lithium borovanadate glass systems, Phys. Chem. Glasses Eur. J. Glass Sci. Technol. Part B 55 (2) (2014) 85–96.
- [27] B. Chen, U. Werner-Zwanziger, M.L.F. Nascimento, L. Ghussn, E.D. Zanotto, J. W. Zwanziger, Structural similarity on multiple length scales and its relation to devitrification mechanism: a solid-state NMR study of alkali diborate glasses and crystals, J. Phys. Chem. C 113 (48) (2009) 20725–20732.
- [28] B. Raguenet, G. Tricot, G. Silly, M. Ribes, A. Pradel, Revisiting the 'mixed glass former effect in ultra-fast quenched borophosphate glasses by advanced 1D/2D solid state NMR, J. Mater. Chem. 21 (44) (2011) 17693–17704.
- [29] D. Larink, H. Eckert, M. Reichert, S.W. Martin, Mixed network former effect in ion-conducting alkali borophosphate glasses: structure/property correlations in the system [M2O] 1/3 [[B2O3) x (P2O5) 1-x] 2/3 (M= Li, K, Cs), J. Phys. Chem. C 116 (50) (2012) 26162–26176.
- [30] D. Wang, J. Zhang, D. Zhang, S. Wan, Q. Zhang, D. Sun, S. Yin, Structural investigation of Li 2 O–B 2 O 3–MoO 3 glasses and high-temperature solutions:

- toward understanding the mechanism of flux-induced growth of lithium triborate crystal, CrystEngComm 15 (2) (2013) 356–364.
- [31] N.A. Sergeev, B.V. Padlyak, M. Olszewski, P. Stepien, B and 7 Li MAS NMR of glassy and crystalline borate compounds, Funct. Mater. 2 (2014) 177.
- [32] M.R. Chialanza, R. Keuchkerian, A. Cárdenas, A. Olivera, S. Vazquez, R. Faccio, J. Castiglioni, J.F. Schneider, L. Fornaro, Correlation between structure, crystallization and thermally stimulated luminescence response of some borate glass and glass-ceramics, J. Non-Cryst. Solids 427 (2015) 191–198.
- [33] T. Ohkubo, E. Tsuchida, T. Takahashi, Y. Iwadate, Ab initio molecular dynamics simulations and GIPAW NMR calculations of a lithium borate glass melt, J. Phys. Chem. B 120 (14) (2016) 3582–3590.
- [34] L.M. Funke, H. Bradtmüller, H. Eckert, Recoupling dipolar interactions with multiple I= 1 quadrupolar nuclei: a 11B {6Li} and 31P {6Li} rotational echo double resonance study of lithium borophosphate glasses, Solid State Nucl. Magn. Reson, 84 (2017) 143–150.
- [35] Y. Kim, K. Morita, Temperature dependence and cation effects in the thermal conductivity of glassy and molten alkali borates, J. Non-Cryst. Solids 471 (2017) 187–194.
- [36] M. de Oliveira Jr, J.S. Oliveira, S. Kundu, N.M.P. Machado, A.C.M. Rodrigues, H. Eckert, Network former mixing effects in ion-conducting lithium borotellurite glasses: structure/property correlations in the system (Li2O) y [2 (TeO2) x (B2O3) 1-x] 1-y, J. Non-Cryst. Solids 482 (2018) 14-22.
- [37] H. R.Fernandes, S. Kapoor, Y.i Patel, K. Ngai, K.L. Levin, Y. Germanov, L. Krishtopa, S. Kroeker, A. Goel, Composition-structure-property relationships in Li2O-Al2O3-B2O3 glasses, J. Non-Cryst. Solids 502 (2018) 142–151.
- [38] V. Montouillout, H. Fan, L. del Campo, S. Ory, A. Rakhmatullin, F. Fayon, M. Malki, Ionic conductivity of lithium borate glasses and local structure probed by high resolution solid-state NMR, J. Non-Cryst. Solids 484 (2018) 57–64.
- [39] A. Ruckman, G. Beckler, W. Guthrie, M. Jesuit, M. Boyd, I. Slagle, R. Wilson, N. Barrow, N. Tagiara, E. Kamitsos, S.A. Feller, C. Bragatto, Lithium ion sites and their contribution to the ionic conductivity of RLI2O-B2O3 glasses with $r \leq 1.85$, Solid State Ion. 359 (2021) 115530.
- [40] B. Topper, E.M. Tsekrekas, L. Greiner, R.E. Youngman, E.I. Kamitsos, D. Möncke, The dual role of bismuth in li2O-bi2O3-b2O3 glasses along the orthoborate join, J. Am. Ceram. Soc. 105 (2022) 7302-7320, https://doi.org/10.1111/jace.18699.
- [41] H. Masai, S. Okumura, T. Ohkubo, T. Yanagida, Luminescence of Sn 2+ center in oxide glass with a tendency toward phase separation, Opt. Mater. Express 7 (8) (2017) 2993–3002.
- [42] I.A. Harris Jr, P.J. Bray, B11 NMR studies of zinc borate compounds and glasses, Phys. Chem. Glasses 25 (3) (1984) 69–75.
- [43] D. Möncke, E.I. Kamitsos, D. Palles, R. Limbach, A. Winterstein-Beckmann, T. Honma, Z. Yao, T. Rouxel, L. Wondraczek, Transition and post-transition metal ions in borate glasses: borate ligand speciation, cluster formation, and their effect on glass transition and mechanical properties, J. Chem. Phys. 145 (12) (2016) 124501.
- [44] K. Januchta, R.L.E. Youngman, L.R. Jensen, M.M. Smedskjaer, Mechanical property optimization of a zinc borate glass by lanthanum doping, J. Non-Cryst. Solids 520 (2019) 119461
- [45] P.J. Bray, M. Leventhal, H.O. Hooper, Nuclear magnetic resonance investigations of the structure of lead borate glasses, Phys. Chem. Glasses 4 (2) (1963) 17.
- [46] A.C. Wright, R.N. Sinclair, D.I. Crimley, R.A. Hulme, N.M. Vedishcheva, B. A. Shakhmatkin, A.C. Hannon, S.A. Feller, B. M Meyer, M.L. Royle, D. L.Wilkerson, Borate glasses, superstructural units and the random network theory 1, Glass Phys. Chem. 22 (4) (1996) 268–278.
- [47] T. Takaishi, J. Jin, T. Uchino, T. Yoko, Structural study of PbO–B2O3 glasses by X-ray diffraction and 11B MAS NMR techniques, J. Am. Ceram. Soc. 83 (10) (2000) 2543–2548.
- [48] A. Saini, A. Khanna, V.K. Michaelis, S. Kroeker, F. González, D. Hernández, Structure–property correlations in lead borate and borosilicate glasses doped with aluminum oxide, J. Non-Cryst. Solids 355 (45–47) (2009) 2323–2332.
- [49] K. I.Chatzipanagis, N.S. Tagiara, E.I. Kamitsos, N. Barrow, I. Slagle, R. Wilson, T. Greiner, M. Jesuit, N. Leonard, A. Phillips, B. Reynolds, B. Royle, K. Ameku, S.

- A. Feller, Structure of lead borate glasses by Raman, 11B MAS, and 207Pb NMR spectroscopies, J. Non-Cryst. Solids 589 (2022) 121660.
- [50] Y. Akasaka, I. Yasui, T. Nanba, Network structure of RO 2B2O3 glasses, Phys. Chem. Glasses 34 (6) (1993) 232–237.
- [51] H. Doweidar, G.M. El-Damrawi, Y.M. Moustafa, Transport properties of semiconducting Fe2O3-PbO-B2O3 glasses, J. Phys. Condens. Matter 6 (42) (1994) 8829
- [52] G. El-Damrawi, F. Gharghar, R.M. Ramadan, Structural studies on new xCeO2· (50− x) PbO· 50B2O3 glasses and glass ceramics, J. Non-Cryst. Solids 452 (2016) 291–296.
- [53] V. Martin, B. Wood, U. Werner-Zwanziger, J.W. Zwanziger, Structural aspects of the photoelastic response in lead borate glasses, J. Non-Cryst. Solids 357 (10) (2011) 2120–2125.
- [54] E. Metwalli, Copper redox behavior, structure and properties of copper lead borate glasses, J. Non-Cryst. Solids 317 (3) (2003) 221–230.
- [55] M.H. Misbah, H. Doweidar, R. Ramadan, M. El-Kemary, Tailoring the structure and properties of iron oxide nanoparticles through the oxygen species of borate glass matrix, J. Non-Cryst. Solids 545 (2020) 120241.
- [56] Y.M. Moustafa, H. Doweidar, G. El-Damrawi, Utilisation of infrared spectroscopy to determine the fraction of the four coordinated borons in borate glasses, Phys. Chem. Glasses 35 (2) (1994) 104–106.
- [57] R. Zhang, M. de Oliveira, Z. Wang, R.G. Fernandes, A.S.S de Camargo, J. Ren, L. Zhang, H. Eckert, Structural studies of fluoroborate laser glasses by solid state NMR and EPR spectroscopies, J. Phys. Chem. C 121 (1) (2017) 741–752.
- [58] A. Bajaj, A. Khanna, B. Chen, J.G. Longstaffe, U.W. Zwanziger, J.W. Zwanziger, Y. Gómez, F. González, Structural investigation of bismuth borate glasses and crystalline phases, J. Non-Cryst. Solids 355 (1) (2009) 45–53.
- [59] K. El-Egili, R. Ghazal, Structural investigation of Fe2O3–Bi2O3–B2O3 glasses, Egypt. J. Chem. 64 (8) (2021) 4069–4079.
- [60] A. Khanna, A. Saini, B. Chen, F. González, C. Pesquera, Structural study of bismuth borosilicate, aluminoborate and aluminoborosilicate glasses by 11B and 27Al MAS NMR spectroscopy and thermal analysis, J. Non-Cryst. Solids 373 (2013) 34–41.
- [61] C.P.E. Varsamis, N. Makris, C. Valvi, E.I. Kamitsos, Short-range structure, the role of bismuth and property-structure correlations in bismuth borate glasses, Phys. Chem. Chem. Phys. 23 (16) (2021) 10006–10020.
- [62] C. Stehle, C. Vira, D. Hogan, S. Feller, M. Affatigato, Optical and physical properties of bismuth borate glasses related to structure, Phys. Chem. Glasses 39 (2) (1998) 83–86.
- [63] H. Maekawa, T. Maekawa, K. Kawamura, T. Yokokawa, The structural groups of alkali silicate glasses determined from 29Si MAS-NMR, J. Non-Cryst. Solids 127 (1998) 53.
- [64] A.M. Peters, F.M. Alamgir, S.W. Messer, S.A. Feller, K.L. Loh, The density of lithium silicate glasses over an extended range of alkali compositions, Phys. Chem. Glasses 35 (5) (1994) 212–215. Numref21 ref.
- [65] C. Larson, J. Doerr, M. Affatigato, S. Feller, D. Holland, M.E. Smith, A29si mas NMR study of silicate glasses with a high lithium content, J. Phys. Condens. Matter 18 (2006) 11323–11331, https://doi.org/10.1088/0953-8984/18/49/023.
- [66] N. Bansal, R. Doremus, Handbook of Glass Properties, Academic Press, London, 1986
- [67] F. Fayon, C. Bessada, D. Massiot, I. Farnan, J.P. Coutures, 29Si and 207Pb NMR study of local order in lead silicate glasses, J. Non-Cryst. Solids (1998), 232 +234403+408.
- [68] S. Feller, G. Lodden, A. Riley, T. Edwards, J. Croskrey, A. Schue, D. Liss, D. Stentz, S. Blair, M. Kelley, G. Smith, S. Singleton, M. Affatigato, D. Holland, M.E. Smith, E. I. Kamitsos, C.P. Varsamis, E. Ioannou, A multispectroscopic structural study of lead silicate glasses over an extended range of compositions, J. Non-Cryst. Solids 356 (6–8) (2010) 304–313.
- [69] American Elements, Bismuth oxide, American elements. (2017). https://www.am ericanelements.com/bismuth-oxide-1304-76-3 (accessed December 26, 2023).
- [70] Bismuth(III) oxide, Bismuth(III) oxide. (n.d.). https://www.chemeurope.com/en/en/cyclopedia/Bismuth%28III%29_oxide.html (accessed December 26, 2023).